united nations
educational, scientific
and cultural
organization

international atomic
energy agency

the
abdus salam
international centre for theoretical physics

SMR.1313 - 2

Summer Colloquium on the Physics of Weather and Climate

Workshop on Land-Atmosphere Interactions in Climate Models

(28 May - 8 June 2001)

Modeling Land Surface Processes in Climate Models: II

"A Review of Modeling Approaches"

Filippo Giorgi
the Abdus Salam ICTP
Physics of Weather & Climate Section
Trieste
ITALY

Modeling land surface processes in climate models: II. A review of modeling approaches

Filippo Giorgi

Abdus Salam International Centre for Theoretical Physics (ICTP)
P.O. Box 586,
34100, Trieste, Italy

2.1. Introduction

In the previous lecture we have seen that, within the context of climate system modeling, the role of what we have called Earth Surface Exchanges Models (or ESEMs) is to provide an interface between the different components of the climate system. In practice, this translates into the following functions: 1) Provide fluxes at the surface-atmosphere interface of net radiation, momentum, sensible heat and water vapor; 2) Describe the energy and water budget of a near surface soil region where biospheric processes are important; 3) Describe the energy and water budget of a vegetative canopy; 4) Describe the cycle of snow formation and melting.

Since the development of the first general circulation models, surface schemes of increasing physical complexity have been developed to carry out these tasks, and presently, over 30 surface process models are available in the literature. The purpose of this lecture is to provide a description of the basic mathematical and physical framework of different modeling approaches. The lecture begins with a brief description of the simplified surface process representation in early climate models (section 2.2). An analysis of more comprehensive models is then presented in section 2.3, and a discussion of problems related to model validation is given in section 2.4. Note that symbols which were defined in Lecture I are not re-defined here.

2.2. Early simplified ESEMs

In the early stages of atmospheric model (AM) development, the surface of the Earth was treated very simply. Basically, the need was simply to provide acceptable values of surface fluxes as lower boundary condition for AMs. Early three-dimensional climate models did not include the diurnal cycle and distinguished only three types of surfaces: land, ocean and ice/snow. These types where generally specified with constant values of albedo, emissivity, drag coefficient and surface wetness factor. The surface skin temperature over

land areas was calculated from an instantaneous energy balance equation

$$(1-\alpha)S_0 + \epsilon I R_D - \epsilon \sigma_B T_g^4 - SH - LH = 0 \tag{1}$$

where SH and LH are given by Eqs. (23) and (24) of Lecture I. Note that a term accounting for the exchange with a deeper soil reservoir is not included in Eq. (1), so that this equation yields realistic average skin temperatures only in the absence of a diurnal insolation cycle. Eq. (1) is of the form $f(T_g) = 0$ and was usually solved via a Newton-Raphson iterative procedure

$$T_g^{(m+1)} = T_g^{(m)} - \frac{f(T_g^{(m)})}{f'(T_g^{(m)})} \tag{2}$$

where (m) is the iteration count. The surface hydrologic cycle was not explicitly described, the specified surface wetness factor β (see Eq. (24) of Lecture I) being essentially treated as a tuning parameter.

Inclusion of the diurnal cycle in AMs required the use of an energy exchange term with a deeper soil resevoir, since the direct use of Eq. (1) would yield excessively large diurnal temperature excursions. One of the most efficient and accurate ways of including this process is the force-restore method originally proposed by Bhumralkar (1975) and Blackadar (1976). In this approach a reservoir temperature T_d is introduced and the surface skin temperature is calculated from the system of equations

$$\frac{\partial T_g}{\partial t} = \frac{c_1 H_s}{\rho_s c_s d_1} - \frac{c_2}{\tau_1}(T_g - T_d) \tag{3}$$

$$\frac{\partial T_d}{\partial t} = -c_3\left[\frac{(T_d - T_g)}{\tau_1} + c_4(T_d - T_{ref})\right] \tag{4}$$

where $\rho_s c_s$ is the soil specific capacity, H_s is the net surface heating, τ_1 is the period of surface heating (i.e. 1 day), d_1 is the soil depth influence by diurnal heating (typically of the order of a few tens of cm), T_{ref} is an annual mean reference temperature and $c_1 - c_4$ are constants. Eqs. (3) and (4) express the condition that the surface temperature is forced by the diurnal surface heating and restores to the reservoir temperature T_d, which in turn restores to the annual mean T_{ref}. The parameters $c_1 - c_4$ can be chosen such that T_g follows a diurnal cycle and T_d follows a seasonal cycle. The force restore method is rather accurate and highly efficient when compared to more complex soil layer models (Deardorff 1978), and still today it is used in advanced surface process schemes.

From the viewpoint of surface hydrology, the use of specified surface wetness factors presents a strong constraint, because it prevents the surface hydrology to reach a dynamical equilibrium with the forcing climate. In particular, this precludes the use of AMs for

simulations of climate and hydrologic regimes different from present and the study of atmosphere-hydrology feedbacks mechanisms. The simplest model of interactive surface hydrology was introduced in the late sixties by Manabe et al. (1969) with the concept of "bucket" model (Fig. 2.1). In this approach it is assumed that the hydrologically active region of soil can be described as a bucket of given water capacity (e.g. 15-20 cm). The bucket fills up if precipitation exceeds evaporation and it is depleted if the opposite occurs. The wetness factor, β, is given by

$$\beta = 1 \qquad s \geq s_c \tag{5a}$$

$$\beta = \frac{s}{s_c} \qquad s \leq s_c \tag{5b}$$

where s is the water content relative to the bucket saturation and s_c is a critical water content. Thus, β increases linearly with s until the critical value is reached and then it is equal to 1. If the maximum capacity of the bucket is reached, the excess water is removed as runoff. The empirical basis for the bucket parameterization resides in diurnally averaged data, therefore the bucket approximation is mostly used in AMs which do not include the diurnal cycle of insolation.

Some of these simple parameterizations of the surface energy and water budgets were sufficient to provide first order surface forcings for early climate models. However, starting in the early eighties, the need for more comprehensive biophysical models of surface processes was recognized for a more realistic description of biosphere-atmosphere interactions. The first biophysically-based ESEMs were developed in the mid-eighties and, since then, such type of surface process schemes have been widely used in climate models. The characteristics of state-of-the-art, biophysically-based ESEMs available in the literature are discussed in the next sections.

2.3. State of the art ESEMs

As mentioned in section 2.1, to date over 30 surface process models have been developed. However, they are in some ways mostly based on two pioneering schemes, the Biosphere-Atmosphere-Transfer Scheme (BATS) of Dickinson et al. (1986, 1993) and the Simple Biosphere model (SiB) of Sellers et al. (1986). Figure 2.2 illustrates the basic sub-components of most state-of-the-art ESEMs: i) A soil model; ii) A vegetation model; iii) a snow model; and iv) a surface runoff model. These sub-components are separately discussed in the following sub-sections.

2.3.1. Soil sub-component

The main purpose of an ESEM soil sub-component is to provide vertical profiles of temperature and soil water content within a soil column of a few meters depth. This is generally considered as the soil zone where biophysical processes (e.g. evapotranspiration) are important, but it can extend a few meters below the depth of the rooting zone. In the absence of strongly sloping surfaces, such as it occurs for the smoothed topographies of climate models, vertical energy and water transfer processes in the top few meters of soil dominate over horizontal transfer. The advent of increasingly powerful computing systems for climate modeling allows today to use explicit vertical layer discretization to numerically solve the equations for the heat and water transport throughout the soil. As illustrative example, we take here the soil component of the Land Surface Exchange scheme (LSX) of Pollard and Thompson (1995).

Vertical energy transport can be described by the equation

$$\frac{\partial}{\partial t}(\rho_s c_s T_s) = \frac{\partial}{\partial z}[k_s \frac{\partial T_s}{\partial z} + \rho_w c_w \overline{s w_s T_w}] \tag{6}$$

where k_s is the heat diffusivity in the soil s is the soil water relative to saturation and ρ_w, c_w, w_s, T_w are the density, specific heat, vertical velocity and temperature of soil water. The vertical coordinate z has origin at the surface and increases downward to reach the total soil depth H_s. The first term to the right hand side of Eq. (6) represents heat transfer by diffusive processes, while the second term describes heat transport by soil water movement. Boundary conditions for the Eq. (6) assume the net surface energy flux at $z = 0$ and relaxation to an average deep temperature reservoir at $z = H_s$.

In describing water movement through the soil, it should first be noted that in most conditions the upper few meters of soil are unsaturated, i.e. they contain both water and air. Once water enters an unsaturated soil it either evaporates or infiltrates downwards due to the effect of gravity and forces arising from interactions between soil and water (e.g. capillarity, Philip 1957). The potential associated with these forces can be measurerd by well-established experimental techniques and can be related to the water content relative to saturation via an empirical power formula (Clapp and Hornberger 1978). As a result, the equation of water movement through an unsaturated soil can be written in terms of the water content relative to saturation as (Pollard and Thompson 1995)

$$p_{or} \frac{\partial s}{\partial t} = \frac{\partial}{\partial z}[-K_w + D_w \frac{\partial s}{\partial z}] \tag{7}$$

where p_{or} is the soil porosity (volume of voids divided by the volume of soil), K_w is the hydraulic conductivity and D_w is the soil moisture diffusivity. Both K_w and D_w are highly non-linear functions of s, given by $K_w = K_{w0} s^{2B+3}$ and $D = K_{w0} \phi_0 B s^{B+2}$, where K_{w0} and ϕ_0 are saturated hydraulic conductivity and water potential and B is an empirical

parameter which varies from ~3 for sand to ~11 for clay. Substituting these expressions in Eq. (7) yields

$$P_{or}\frac{\partial s}{\partial t} = \frac{\partial}{\partial z}[-K_{w0}s^{2B+3} + K_{w0}\phi_0 B s^{B+2}\frac{\partial s}{\partial z}] \tag{8}$$

In Eq. (8), the first term to the r.h.s. represents water gravitational drainage while the second describes water diffusion. Boundary conditions for Eq. (8) assume water net flux due to precipitation, snow melt, runoff and evaporation at $z = 0$ and free drainage or zero permeability at $z = H_s$.

The particular aspect of Eq. (8) is that it is highly non linear in s. In practice, this implies that in the numerical solution of this equation, explicit schemes become rapidly unstable as s approaches unity. In order to be able to simulate the motion of wetting fronts associated for example to heavy precipitation events, it is thus necessary to devise implicit schemes which remain stable also when s is close to 1.

In summary, Eqs. (6) and (8) describe the energy and water movement in the unsaturated soil zone with the upper boundary condition given by the net energy and water flux at the top of the soil layer. Soil ice formation, important for the simulation of permafrost, can be included by assuming that, when the temperature of a given soil layer goes below the freezing point, an amount of ice is formed whose release of heat of fusion brings the temperature of the layer back to 0°C.

The main issue in the use of soil layer models is the number of layers necessary to simulate accurately temperature and water vertical profiles. Numerical experiments indicate that at least 6-10 layers in the top few meters of soil are generally required (Dickinson 1984).

2.3.2 Vegetation sub-component

Most state-of-the-art ESEMs include bio-physical vegetation processes by describing vegetation as a one layer canopy or as an upper canopy layer (trees) overlying a lower canopy layer (grass and short shrubs). It is useful, however, to introduce a general formalism for a canopy of N_V layers. The basic set of equations in a layered canopy model is aimed at calculating foliage temperature, T_f, canopy air temperature T_c and canopy air specific humidity, q_c. These quantities are strongly coupled to each other and eventually determine the energy and water exchange with the atmosphere and with the soil. In many models it is assumed that both foliage and air canopy have negligible heat and water capacity. With this assumption, at each layer ($i = 2, N_V - 1$) a set of three balance equations can be defined:

Energy balance for the canopy foliage

$$S_0^i + IR_N^i - k_{f,c}^i(T_f^i - T_c^i) - Le_{f,c}^i(q_s(T_f^i) - q_c^i) = 0 \tag{9}$$

Energy balance for the air canopy

$$k^i_{f,c}(T^i_f - T^i_c) + k^{(i,i+1)}_c(T^{i+1}_c - T^i_c) + k^{(i,i-1)}_c(T^{i-1}_c - T^i_c) = 0 = 0 \tag{10}$$

Water balance for the air canopy

$$e^i_{f,c}(q_s(T^i_f) - q^i_c) + k^{(i,i+1)}_c(q^{i+1}_c - q^i_c) + k^{(i,i-1)}_c(q^{i-1}_c - q^i_c) = 0 \tag{11}$$

In Eqs. (9)-(11) S^i_0 and IR^i_N are the net solar and infrared fluxes at the foliage surface, respectively, $k_{f,c}$ is a foliage-canopy air heat transfer coefficient, $e_{f,c}$ is a transfer coefficient for transpiration, L is the latent heat of evaporation, and k_c is a heat and water vertical turbulent transfer coefficient within the canopy.

The third and fourth terms in Eq. (9) and the first terms in Eqs. (10)-(11) are the sensible and latent heat (or water vapor) exchanges between canopy foliage and canopy air. Similar to the surface-atmosphere exchanges discussed in Lecture I, these fluxes can be expressed as the product of a transfer coefficient times a difference in potential, therefore the transfer coefficients can also be interpreted as inverse of resistances. The second and third terms in Eqs. (10)-(11) are the energy and water exchanges between canopy air layers.

At i = 1 (next to the ground) Eq. (9) remains unaltered, but Eqs. (10)-(11) become

$$k^i_{f,c}(T^i_f - T^i_c) + k^{(i,i+1)}_c(T^{i+1}_c - T^i_c) + k_{c,g}(T_g - T^i_c) = 0 \tag{12}$$

$$e^i_{f,c}(q_s(T^i_f) - q^i_c) + k^{(i,i+1)}_c(q^{i+1}_c - q^i_c) + k_{c,g}\beta_g(q_s(T_g) - q^i_c) = 0 \tag{13}$$

where $k_{c,g}$ is the exchange coefficient between ground and lower canopy (same for heat and moisture) and β_g is a ground wetness factor. For $i = N_V$ (top canopy layer)

$$k^i_{f,c}(T^i_f - T^i_c) + k^{(i,i-1)}_c(T^{i-1}_c - T^i_c) + k_{c,a}(T_a - T^i_c) = 0 \tag{14}$$

$$e^i_{f,c}(q_s(T^i_f) - q^i_c) + k^{(i,i-1)}_c(q^{i-1}_c - q^i_c) + k_{c,a}(q_a - q^i_c) = 0 \tag{15}$$

where $k_{c,a}$ is the exchange coefficient between the top canopy layer and the bottom AM level. In addition, Eqs. (9)-(15) need be coupled with an equation for the surface ground temperature underlying the canopy

$$S_{0,g} + IR_{N,g} - k_{c,g}(T_g - T^1_c) - Lk_{c,g}\beta_g(q_s(T_g) - q^1_c) = 0 \tag{16}$$

where $S_{0,g}$ and $IR_{N,g}$ are the solar and infrared net fluxes at the ground surface.

The first difficulty which arises in the solution of the system (9)-(16) is the specification of the various radiative and turbulence transfer terms appearing in it. The net solar and infrared contributions S^i_0 and IR^i_N can be calculated once the thermal infrared emission

and the solar extinction coefficients are know for each vegetation layer. The emissions can be expressed as exponential functions of the leaf area index in a layer, L_i, (Sellers et al. 1986)

$$\epsilon_i = 1 - e^{-L_i/2\overline{\mu}} \tag{17}$$

where $\overline{\mu}$ is the average inverse diffuse optical depth. Once the emissivities are known, the terms IR_N^i in Eqs. (9)–(16) can be calculated from the absorption-emmissions of the different layers.

A common approach to the calculation of solar fluxes within the canopy has been to use a two-stream approximation accounting for multiple reflections by leaves and radiation trapping by dense canopies (Dickinson 1983, Sellers et al. 1986). The system of two-stream equations regulating the upward and downward solar fluxes are

$$-\overline{\mu}\frac{dS^{\uparrow}}{dL} + (1-(1-\gamma)\omega)S^{\uparrow} - \omega\gamma S^{\downarrow} = \omega\gamma_0\overline{\mu}\frac{G}{\mu}D_0 e^{-GL/\mu} \tag{18}$$

$$\overline{\mu}\frac{dS^{\downarrow}}{dL} + (1-(1-\gamma)\omega)S^{\downarrow} - \omega\gamma S^{\uparrow} = \omega(1-\gamma_0)\overline{\mu}\frac{G}{\mu}D_0 e^{-GL/\mu} \tag{19}$$

where $S^{\uparrow}$ and $S^{\downarrow}$ are the hemispheric upward and downward diffuse fluxes, μ is the cosine of the incident direct beam and D_0 is its intensity, $G(\mu)$ is the relative projected leaf area in direction μ, ω is a leaf scattering coefficient and γ, γ_0 are the backscatter parameters of a leaf for diffuse and direct beam, respectively. The intensity of the direct beam is $D_0 e^{-G\times LAI/\mu}$. The various parameters appearing in Eqs. (18)-(19) can be calculated as described in Dickinson (1983) and Sellers et al. (1986).

With the boundary conditions $S^{\downarrow} = S_0$ at the canopy top $L = 0$ and $S^{\uparrow} = \alpha_d D_0 e^{-GLAI/\mu} + \alpha_I S^{\downarrow}$ (where α_d and α_I are the direct and diffuse surface albedoes) at the canopy bottom ($L = LAI$) the solutions to the system (18)-(19) are

$$S^{\uparrow} = a_1 e^{-GL/\mu} + a_2 e^{-a_3 L} + a_4 e^{-a_3 L} \tag{20}$$

$$S^{\downarrow} = a_5 e^{-GL/\mu} + a_6 e^{-a_3 L} + a_7 e^{-a_3 L} \tag{21}$$

where $a_1 - a_7$ are algebraic combinations of the coefficients of the equations (Sellers 1985). Once the upward and downward fluxes are calculated as a function of leaf area index, the term S_0^i in Eq. (9) is given by the net flux absorbed by each layer. Note that Eqs (18)-(21) can be used to calculate the canopy albedo as $S^{\uparrow}(0)/S^{\downarrow}(0)$.

More difficult is the treatment of turbulent transfer coefficients appearing in Eqs. (9)-(11). The canopy-to-atmosphere transfer coefficient is usually expressed in terms of the bulk drag coefficient and the lowest AM level wind speed, i.e. $k_{c,a} = C_d V_a$ (see Eqs. (20)-(24) of Lecture I). Therefore, in the presence of a vegetative canopy the surface-atmosphere

fluxes of momentum, heat and water vapor needed as AM lower boundary conditions are given by

$$\tau_{0,u} = \rho k_{c,a} u_a \tag{22}$$

$$\tau_{0,v} = \rho k_{c,a} v_a \tag{23}$$

$$SH = \rho c_p k_{c,a} (T_c - T_a) \tag{24}$$

$$LH = \rho L \; k_{c,a} (q_c - q_a) \tag{25}$$

The transfer coefficients between foliage and canopy air have been determined experimentally to be proportional to the square of the ratio of wind within the canopy and typical size of the foliage elements (Sellers et al. 1986), while the transfer coefficient between canopy air and ground is proportional to the canopy wind close to the surface (Brutsaert 1978). The vertical transfer coefficients within the canopy have also been estimated experimentally (for momentum) for different vegetation types and are proportional to the wind within the canopy. Therefore, solution of the system (9)-(16) requires knowledge of the canopy vertical wind profile. For this purpose, observed exponential wind profiles have been used (Brutsaert 1978) or simple diffusive models such as that of Sellers et al. (1986). These models assume that the momentum diffusivity is proportional to the wind speed and that the vertical gradient of momentum flux, (τ), is proportional to the square of the wind speed, i.e.

$$\frac{d}{dz}(\frac{\tau}{\rho}) = Cu^2 \tag{26}$$

$$\frac{\tau}{\rho} = (Du)\frac{du}{dz} \tag{27}$$

whose solution is

$$u(z)^2 = Ae^{\lambda z} + Be^{-\lambda z} \tag{28}$$

where $\lambda = (2C/D)^{0.5}$ and A and B are integration constants adjusted to satisfy boundary conditions at the top and bottom of the canopy.

The second difficulty in the solution of the system (9)-(16) is that this is highly non-linear. Non-linearities enter the infrared radiative term, the temperature dependency of the saturation specific humidity and the stability correction of the canopy-to-atmosphere transfer coefficient. An effective way to solve this system is to use an iterative method in which the non-linear terms are linearized around the values at the previous iteration. This leads to a linear system of equations for T_f, T_c, and q_c at the various model levels, which can be solved, for example, via Gaussian elimination.

In most situations, the complexity of the system (9)-(16), the uncertainty in the within-canopy transfer coefficients and the lack of data for model calibration and validation, make the use of the full N_V-layered system unpractical in climate models. Therefore, as we

already mentioned, most often the vegetation is treated as one bulk layer and the system (9)-(16) reduces to three coupled equations in three unknowns.

An important term in Eq. (9), which we have not studied yet, is the foliage evaporative flux $e_{f,c}(q_s(T_f) - q_c)$. This is the sum of two contributions, tranpiration from dry foliage surfaces and evaporation of intercepted water. These two contributions are separately treated in the next sub-sections.

2.3.2.1. Transpiration

Transpiration is a complex process which involves knowledge of the physiological behaviour of plants. In the transpiration process, water is uptaken from the soil by the plant rooting system, it is transported throughout the plant vascular system and it is transpired mostly through the stomatal pores, which lie on the leaf surface (some transpiration takes place through the leaf cuticles). A resistance analogy scheme for the transpiration process is depicted in Fig. 2.3.

Water vapor inside a leaf is kept at or near its saturation value, for otherwise the leaf would desiccate. Therefore the transpiration (demand) flux (TR_{dem}) is given by

$$TR_{dem} = e_{f,c}(q_s(T_f) - q_c) = r_f^{-1}(q_s(T_f) - q_c) \tag{29}$$

where r_f is the leaf resistance. Through the resistance analogy of Fig.2.3 r_f is given by the sum of r_b, the aerodynamic resistance to vapor transport from the leaf surface to the canopy (i.e. $k_{f,c}^{-1}$), and the stomatal resistance r_s, i.e. the resistance to flow across the stomatal pores. Thus

$$TR_{dem} = (r_b^{-1} + r_s^{-1})(q_s(T_f^i) - q_c^i) \tag{30}$$

TR_{dem} in Eq. (30) represents the water demand under no soil moisture stress. The aerodynamic resistance has already been described in section 2.3.2. The stomatal resistance depends on the density and opening of the pores, where the latter in turn depends on environmental parameters such as the amount of photosynthetically active radiation (PAR), temperature and vapor pressure deficit, vpd, between leaf and canopy air. These dependences are usually expressed as

$$r_s = min[r_{s,max}, r_{s,min} \times f(PAR) \times f(T) \times f(vpd)] \tag{31}$$

where $r_{s,min}$ and $r_{s,max}$ are vegetation-dependent minimum and maximum values of stomatal resistance. Parameterizations of the functions in the r.h.s. of Eq. (31) are given for example by Dickinson et al. (1993). A parameterization of stomatal resistance, which more explicitly links stomatal physiology with the rate of foliage photosynthesis is given by Collatz et al. (1991) and Sellers et al. (1992).

The evaporative demand must be consistent with the maximum transpiration the plant can support given the soil moisture conditions, or soil water supply. The soil water supply depends on the difference between the soil and leaf water potential divided by the root resistance r_c, which depends on the total length of root per unit area and the internal plant resistance per unit root length. For very dry soil, the resistance to water diffusion from the soil to the roots also plays a significant role. Dickinson et al. (1993) lump all these contributions into a simple parameterized expression of the water supply flux

$$TR_{sup} = \Gamma_0 \sum_i R_t^i (1 - W_{LT}^i) \tag{32}$$

where Γ_0 is an experimentally-derived maximum transpiration rate which can be sustained by the vegetation, R_t^i is the fraction of roots in a given soil layer and W_{LT}^i is a soil dryness (or plant wilting) factor for the soil layer. W_{LT} varies as a power function of the parameter B in Eq. (8) from 1 at saturation to 0 at a soil water threshold for plant wilting. The minimum between (30) and (32) is taken as the transpiration value.

2.3.2.2. Interception and re-evaporation

Interception and re-evaporation of precipitation by the canopy foliage can be an important component of the surface water cycle. Typical values of reevaporation of intercepted precipitation are in the range of 10–50%, depending on rainfall and LAI. In addition, the film of water that form over leaves inhibits transpiration. Most state-of-the-art ESEMs include an equation for intercepted water on vegetation of the type

$$\frac{dW_l}{dt} = \frac{P}{LAI} - E' - \frac{W_l}{\tau_{drip}} \tag{33}$$

where W_l is the intercepted water per unit LAI, E' is evaporation of water on leaves (given by $r_b^{-1}(q_s(T_f) - q_c)$ in Eq. (9)) and τ_{drip} is a water dripping time.

The fraction of the foliage actually covered by intercepted water is generally parametierized with a simple formula such as

$$f_{wet} = min[f_{max}, W_l/W_l^{max}] \tag{34}$$

where f_{max} and W_l^{max} are specified constant values. Once the fraction of wetted foliage area is calculated, the total flux into the canopy from the foliage in Eq. (9) is given by

$$e_{f,c}(q_s(T_f) - q_c) = f_{wet}E' + (1 - f_{wet})TR \tag{35}$$

2.3.3. Snow sub-component

In this section we give two examples of snow models of increasing complexity. In the early climate models the snow cover amount (in mm of equivalent liquid water), H_{sn} was calculated from the equation

$$\frac{\partial H_{sn}}{\partial t} = P_{sn} - E_{sn} - S_m \tag{36}$$

where P_{sn} is snow fall E_{sn} is snow sublimation and S_m is snow melt. Snow fall is calculated by assuming that if the temperature at the bottom AM level is less than 0°C, or if snow cover exists at a given point, the model precipitation is in the form of snow. The snow temperature is not explicitly carried, but it is blended within the temperature calculation of a surface soil layer by merging snow and soil heat capacities, modifying the surface roughness to that of snow and assuming that only sublimation occurs. The snow melt rate is calculated from the surface energy balance as

$$S_m = L_f^{-1}[S_0 + IR_N - SH - LH] \tag{37}$$

where L_f is the latent heat of fusion. If in the presence of snow cover the r.h.s. of Eq. (37) is positive and the soil temperature is greater than 0°, the heat necessary to bring the soil temperature back to 0° is calculated. Snow melt is then the minimum of this calculated heat divided by L_f, the r.h.s. of (37) and $\Delta t \times H_{sn}$.

An example of more advanced snow module is that of LSX (Pollard and Thompson 1995). In this model, the snowpack is represented by a vertical adaptive layer grid. This consists of dividing at each time step the total snow depth H_{sn} in a pre-selected number of layers N_{sn}. The depth of the top layer h_{sn}^1 is assumed to be constant and the depth of the remaining layers is given by

$$h_{sn}^i = \frac{H_{sn} - h_{sn}^1}{N_{sn} - 1} \tag{38}$$

In this way, the depth of the layers varies with time depending on H_{sn}. H_{sn} is given by Eq. (36) and the temperature of the snow layers is calculated from a vertical diffusion equation similar to Eq. (6) forced at the top by the net energy flux (r.h.s. of Eq. (37)) and at the bottom by the conductive energy flux between snow and underlying soil. When at a given layer the snow temperature goes above the melting point, snow melt is calculated as the amount of melted snow necessary to bring the temperature of the layer back to 0°C.

This model also requires calculation of a fractional snow cover f_{sn}. This is calculated by assuming a minimum total snow depth of $N_{sn} \times h_{sn}^1$, which leads to

$$f_{sn} = min[1., \frac{H_{sn}}{N_{sn} h_{sn}^1}] \tag{39}$$

Based on (39), when f_{sn} is less than 1, H_{sn} is set to $N_{sn} \times h^1_{sn}$. When it is snowing, the quantity

$$\Delta f_{sn} = \frac{P_{sn}\Delta t}{N_{sn}h^1_{sn}} \tag{40}$$

is appended to the side of existing snow at each time step Δt. When the fractional snow cover becomes 1, further snow is accumulated on top of existing one. Different calculations of fractional snow cover as a function of snow depth and surface characteristics can also be found in other schemes (e.g Dickinson et al. 1993). Snow density is mostly assumed constant, except for a few schemes which include a snow density prognostic equation based on self-loading densification (e.g. Pitman et al. 1991). Snow albedo can either assumed to be constant or can be a function of snow age (Dickinson et al. 1993) and snow granular structure (Pitman et al. 1991).

2.3.4. Surface runoff sub-component

Surface runoff Rn is one aspect of present ESEMs which is still highly parameterized in ways not very dissimilar from those of early bucket models. This is mostly because of the complexity of the surface runoff process, which depends critically on the forcing climate, terrain morphology and soil water movement within the soil. Therefore, many ESEMs still treat surface runoff essentially as a residual term necessary to balance the water budget. A typical example of the crudeness of the runoff parameterization in ESEMS used for climate studies is that of BATS, in which the runoff rate is simply assumed to be proportional to the rainfall+snowmelt rate times a power function of the soil water content relative to saturation.

Only recently, more elaborate representations of the surface runoff process, based more firmly on surface hydrologic principles, have been included in ESEMs. A representative example is given by the runoff parameterizations of Famiglietti et al. (1995). Two primary processes contribute to the generation of surface runoff: saturation excess runoff and infiltration excess runoff. Saturation excess runoff prevails when precipitation occurs on saturated soils. In this case most of the precipitation cannot be uptaken by the soil and goes into surface runoff. Infiltration excess runoff occurs when the soil is unsaturated but the precipitation rate exceeds the maximum infiltration capacity of the soil i^*, i.e. the maximum rate at which precipitation can infiltrate the soil column. Therefore

$$Rn = P \qquad s = 1 \tag{41a}$$

$$Rn = P - i^* \qquad s < 1 \tag{41b}$$

where s is the soil water content relative to saturation in a near surface soil layer. The main issue in this parameterization is to calculate the infiltration capacity i^*. One possibility

is to calculate the infiltration rate directly from Eq. (7) by assuming a layer of saturated soil ($s = 1$) overlying the top soil model layer. This assumes that the numerical scheme used to solve Eq. (7) is capable of handling the downward motion of the wetting front. Famiglietti et al. (1995), as well as Bonan (1995), make use of the equation

$$i^* = \frac{1}{2}\phi_0 t^{-1/2} + cK_0 \tag{42}$$

where ϕ_0 and K_{w0} are the saturated soil suction and hydraulic conductivity of Eq. (7), t is time since the onset of infiltration, and c is a dimensionless constant. Eq. (42) is based on the solution by Philip (1957) of the vertical soil water diffusion equation for infiltration from a saturated surface into a soil of initially uniform moisture content.

While Eqs. (41)-(42) can perhaps give better (or at least more physically based) representations of the generation of surface runoff at a given location than early simplified schemes, the parameterization of runoff is complicated by the fact that this is a basin-wide distributed process which depends on soil properties, surface morfology and soil water content and movement throughout the basin. Possibly, only the use of full basin-hydrology models coupled to ESEMs may provide very accurate simulation of timing and amounts of basin-wide runoff. However, simplified parameterizations such as those discussed here might still be able to provide realistic first order estimates of the partitioning of precipitation into runoff and evaporation.

2.4. Model Testing and Validation

Testing and validation of ESEMs can take place at different levels: i) ESEMs can be run in stand alone mode, driven by observed meteorological fields, and the output can be in turn compared to actual observations; ii) the sensitivity of ESEMs to relevant parameter values can be studied; iii) the performance of different ESEMs can be intercompared using the same driving fields; and iv) the performance of ESEMS can be evaluated when coupled with AMs. All of the over 30 currently available ESEMs have undergone at least some of these testing phases and a multitude of articles have been published on ESEM testing, a review of which is beyond the purpose of this lecture. It is useful, however, to provide some general considerations on the performance of ESEMs and problems related to ESEM validation.

Validation of ESEMs is difficult because they usually include a large number of empirical parameters and because there is little available observations for this purpose. Figure 2.4 shows an example of how a state-of-the-art ESEM (the SiB model) can closely reproduce observed fluxes of net radiation, sensible heat and latent heat at the surface when driven by observed climatological fields. This is in some ways not surprising, since the

ESEM parameters can be tuned to yield good simulations of given observed datasets. The issue is to validate ESEMs in a variety of configurations and forcing conditions.

Perhaps the primary framework today available for ESEM validation is the Project for Intercomparison of Land Process Schemes, or PILPS (Pitman et al. 1993). The main purpose of this project is to intercompare present ESEMs under controlled conditions with the goal of i) quantify model differences; ii) determine the importance of these differences for various applications; iii) understand the causes of the differences in terms of theoretical basis for the parameterizations, numerical implementation and coding thereof, and choice of parameters and parameter values. The project has so far been organized in two phases, both of which entail running the ESEMs in stand alone mode driven by specified climatic forcings. In the first phase, the climatic forcing is obtained from output of a GCM simulation for three surface types, tropical rainforest, midlatitude grassland and high latitude tundra. In the second phase, observed data are used for model forcing and validation. Two datasets are presently being used, one for a grassland site located in Cabauw, The Nederlands, and one for a site of soya crop in the HAPEX-MOBILHY experiment (Andre et al. 1986). Care is taken so that the parameter setting is done as to keep as much consistency as possible between different models.

A preliminary analysis of the results from the phase I of the PILPS project has been carried out leading to the main conclusion that current land surface schemes present significant differences in the partitioning of net radiant energy between sensible and latent heat fluxes: ranges as large as 100 W/m^2 exist in annual averages and can be larger on shorter time scales. Soil moisture calculations differ considerably from model to model and many land-surface schemes exhibit multi-year spin-up timeframes. Examples of the range in model response for the simulation of the annual cycle of effective skin temperature, sensible heat flux, latent heat flux, soil moisture content of the top 10 cm layer and total runoff for a tropical forest surface are shown in Figs. 2.5a-e.

These results indicate that still a relatively high level of uncertainty is present in the simulation of surface processes by today's ESEMs. Identifying the causes for the range found in inter-model response is difficult, because of the large number of model parameters and the differences in model formulations and set up. The effects that the use of different ESEMs has on climate models is also difficult to quantify. Changes of a few to several tens of W/m^2 in surface fluxes are sufficient to affect the surface climatology of atmospheric models, with temperature responses of a few to several degrees and precipitation responses up to a few tens of percent (Dickinson 1992, Seller 1992). Overall, however, the simulation of large scale structures of the general circulation in mid and upper troposphere and above is not very sensitive to the use of different surface schemes (Dickinson, pers. comm.).

2.5. Summary considerations

In this lecture a review is given of different approaches to surface modeling, from the early highly parameterized model formulations to state-of-the-art ESEMs which include attempts to describe the basic biophysical processes which regulate the surface water and energy budgets. State-of-the-art ESEMs have reached a high level of complexity, a level that is considered sometimes excessive when compared to other physics representations in climate models. In lecture I we have seen, however, that within the context of climate system modeling, ESEMs assume a central interfacing role, so that they need to describe the complex range of processes which determine the interactions between the atmosphere, the biosphere and the hydrosphere.

Many different ESEMs are today available, with performances which are surprisingly different from each other, given that they mostly derive from a few basic schemes. A strong effort needs to be carried out to understand their differences and their sensitivity to the many parameters involved in each model, and the PILPS project is an important step towards this goal. In addition, a critical need is there today to assemble more observational datasets for model validation, either through field campaigns or through the use of remotely sensed data.

One of the main areas of model uncertainty resides in the partitioning of precipitation into evaporation and runoff, and in the partitioning of energy into latent and sensible heat. This partitioning depends on surface morphology and characteristics which are spatially variable on scales much smaller than those resolved by current climate models. The issue of the representation of surface heterogeneity, which is examined in the next lecture, is thus central to improving surface modeling.

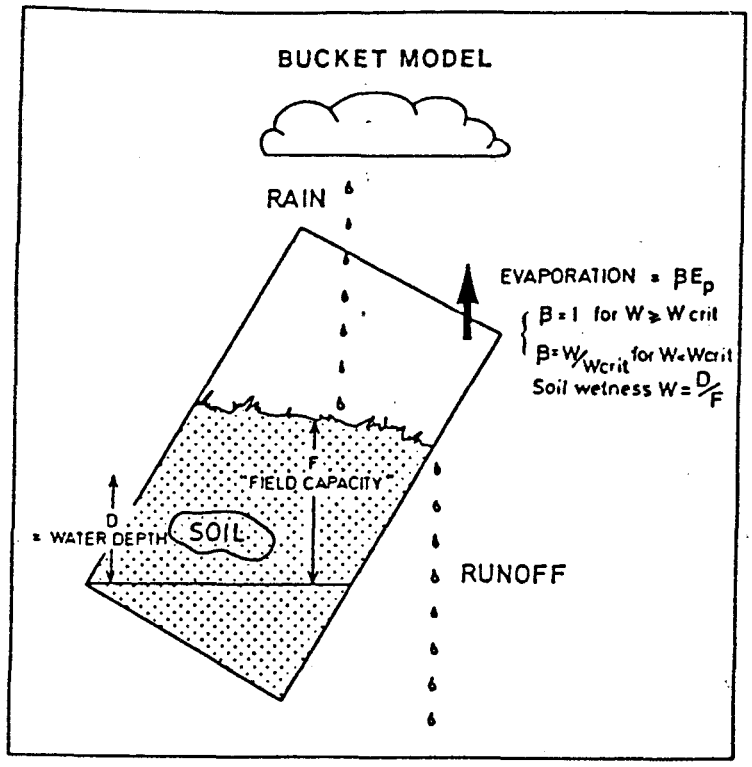

Fig. 2.1 Schematic representation of the bucket model

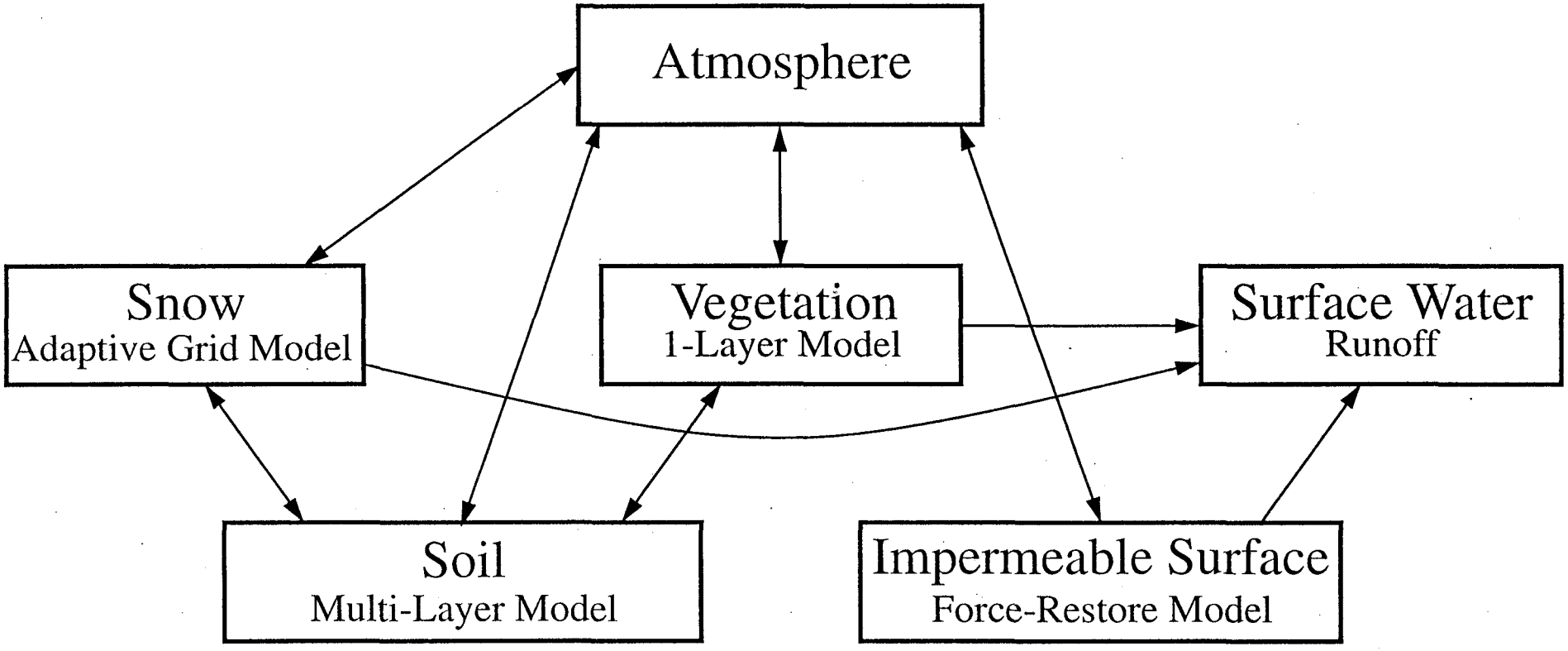

2.2 Different components of an ESEM (Earth surface exchange mode)

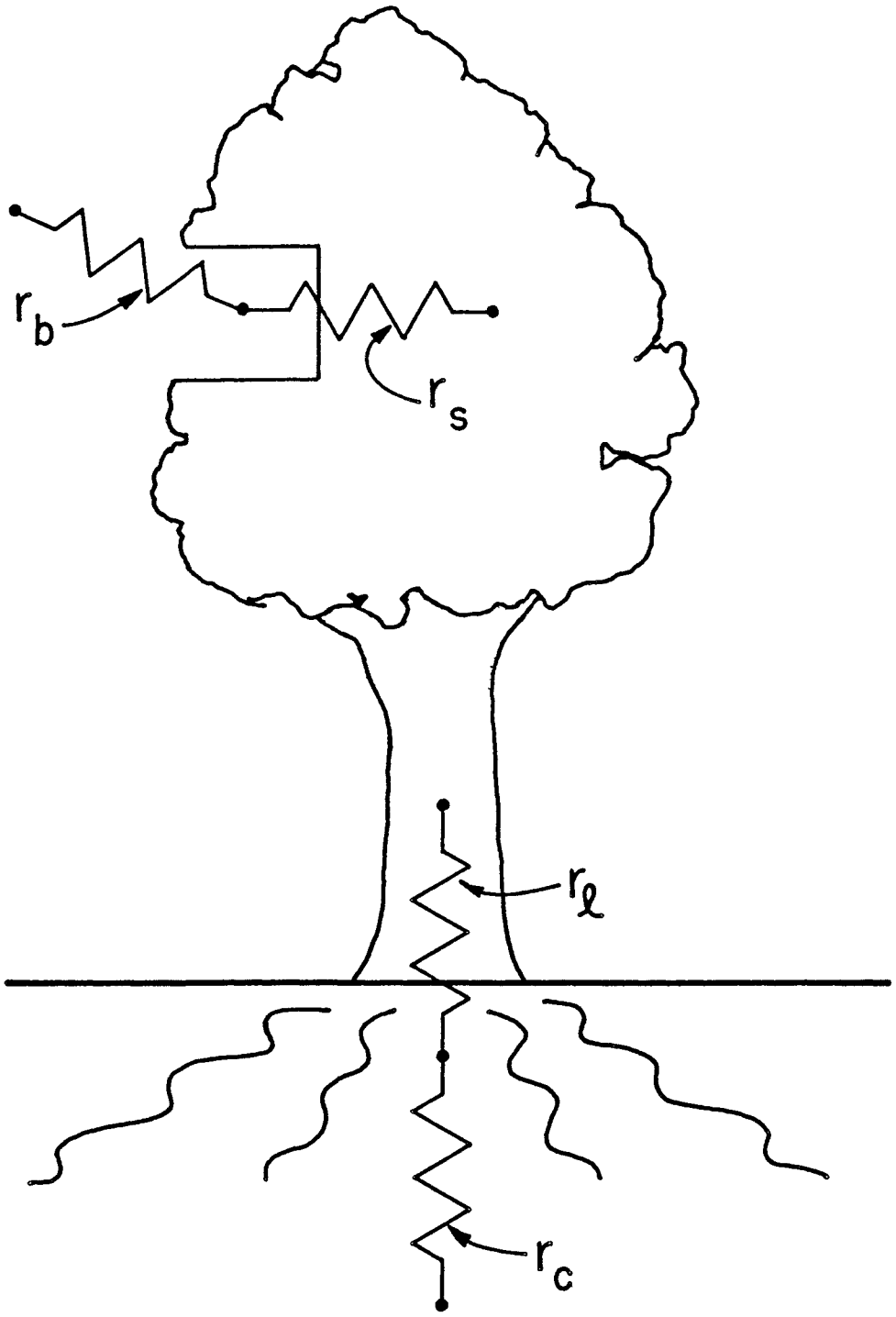

Figure 2.3 Water transfer resistance network for the transpiration process. r_b = aerodynamic resistance, r_s stomatal resistance, r_l resistance to transfer from the roots to the leaves, r_c root resistance.

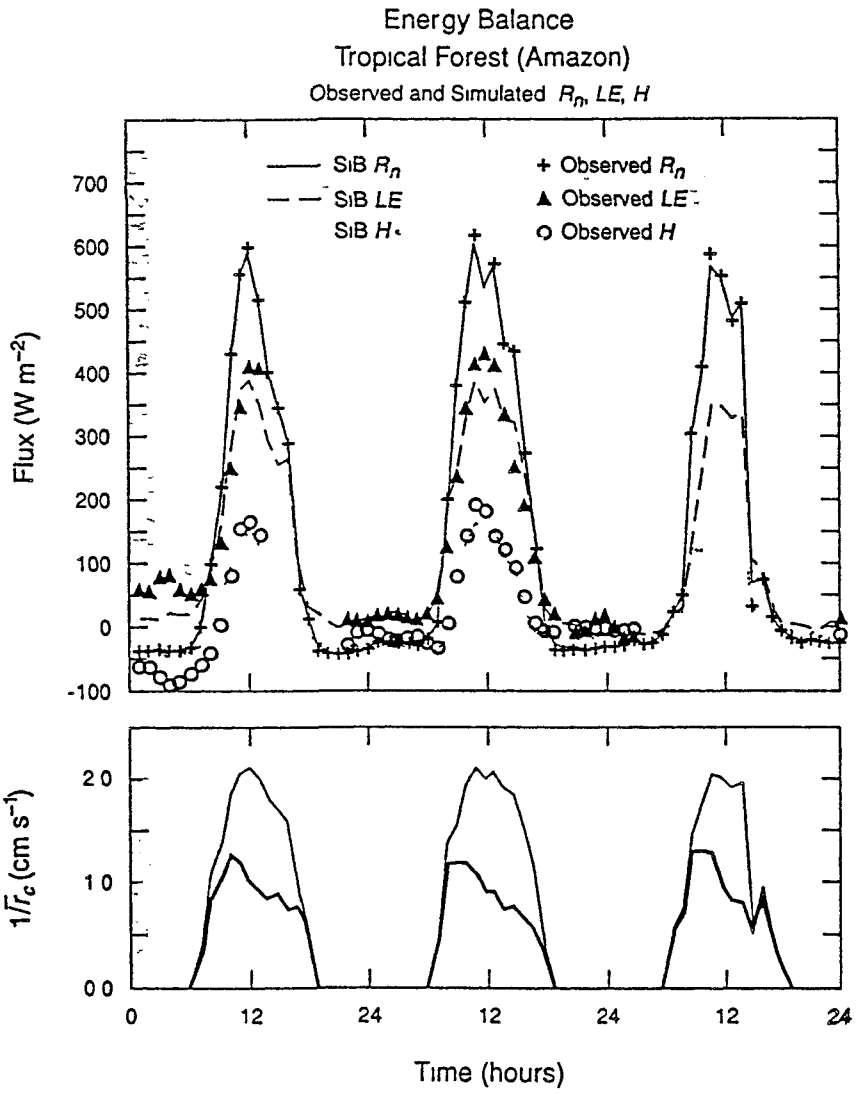

Figure 2.4 Comparison of observed and simulated net radiative, latent heat and sensible heat fluxes for a tropical forest site (From Sellers 1992)

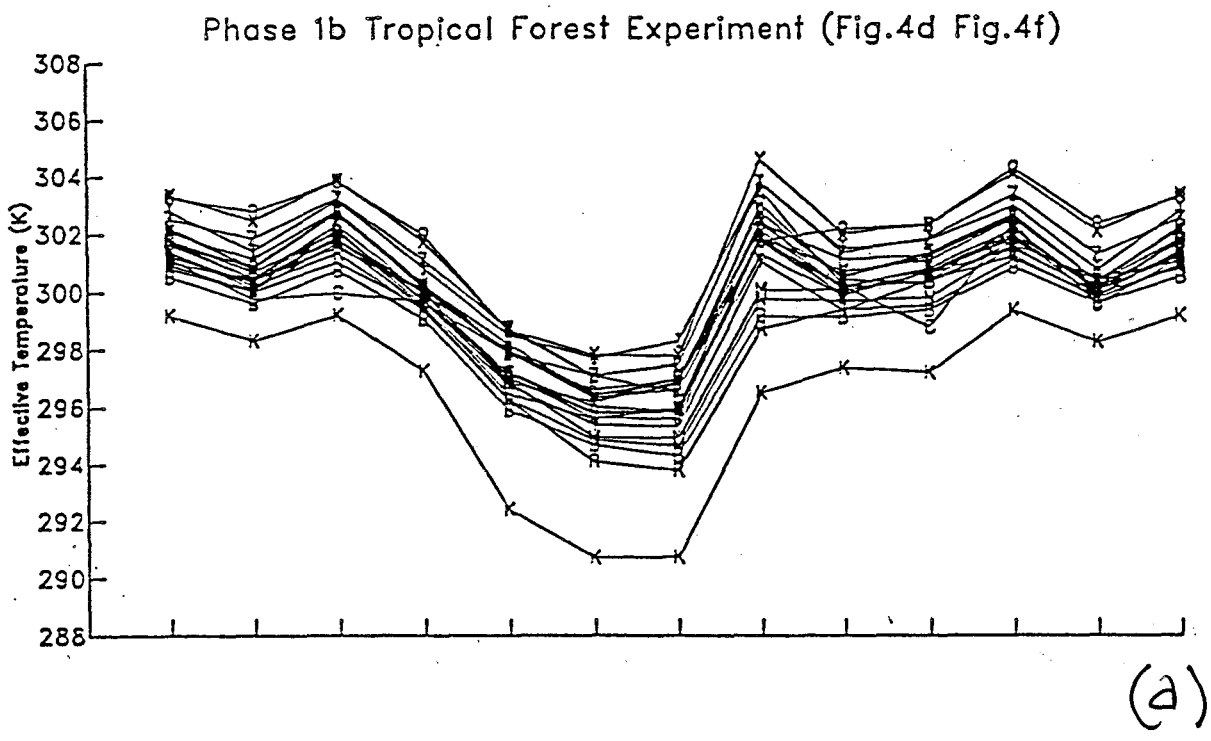

Figure 2.5 Simulated annual cycle of (a) Effective temperature, (b) latent heat flux, (c) sensible heat flux, (d) total runoff, and (e) water content of the upper soil layer for various models in the PILPS experiment.

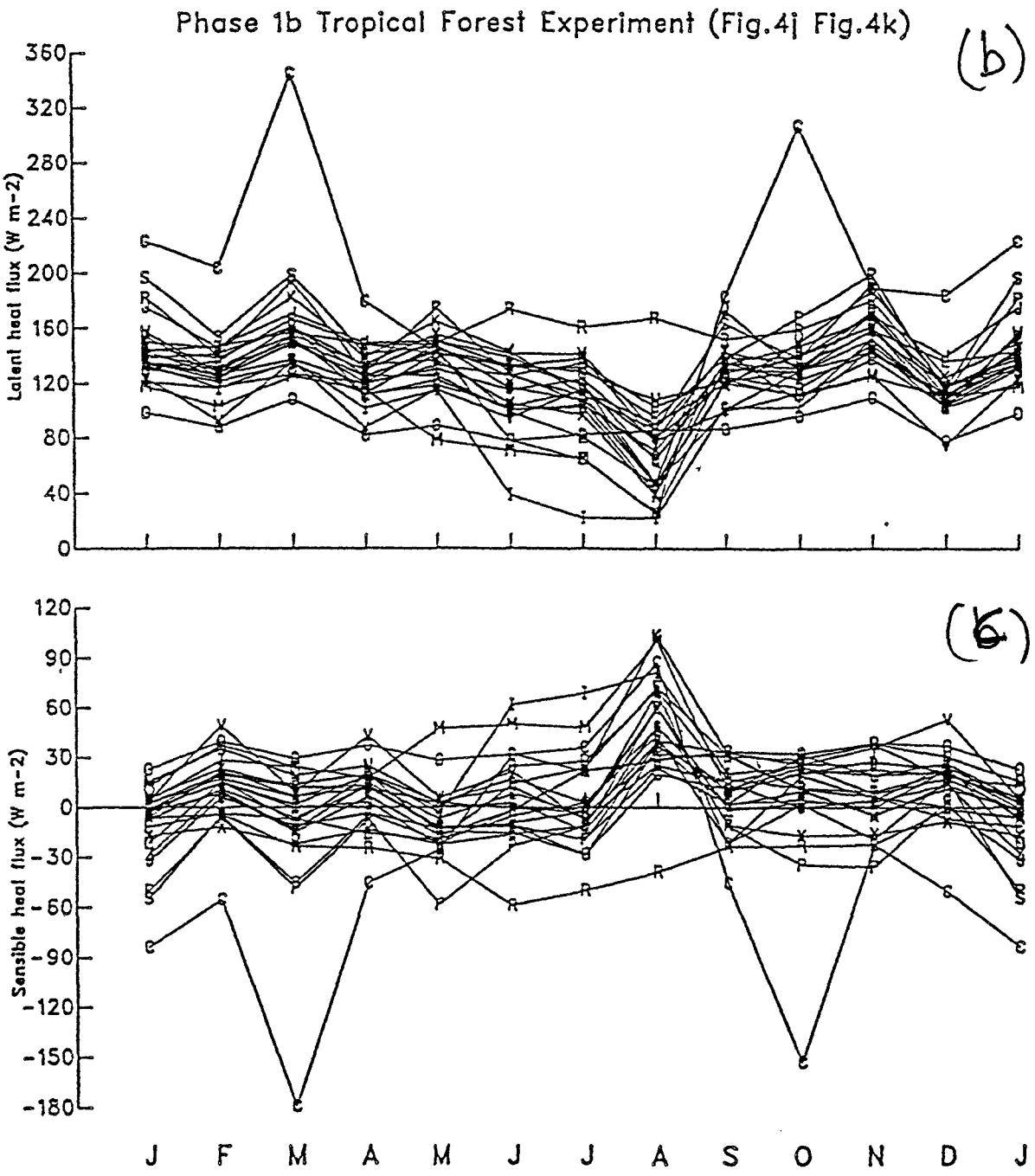
Phase 1b Tropical Forest Experiment (Fig.4j Fig.4k)
(b)
Latent heat flux (W m-2)
360
320
280
240
200
160
120
80
40
0
(c)
Sensible heat flux (W m-2)
120
90
60
30
0
-30
-60
-90
-120
-150
-180
J F M A M J J A S O N D J

Fig. 2.5 (b), (c)

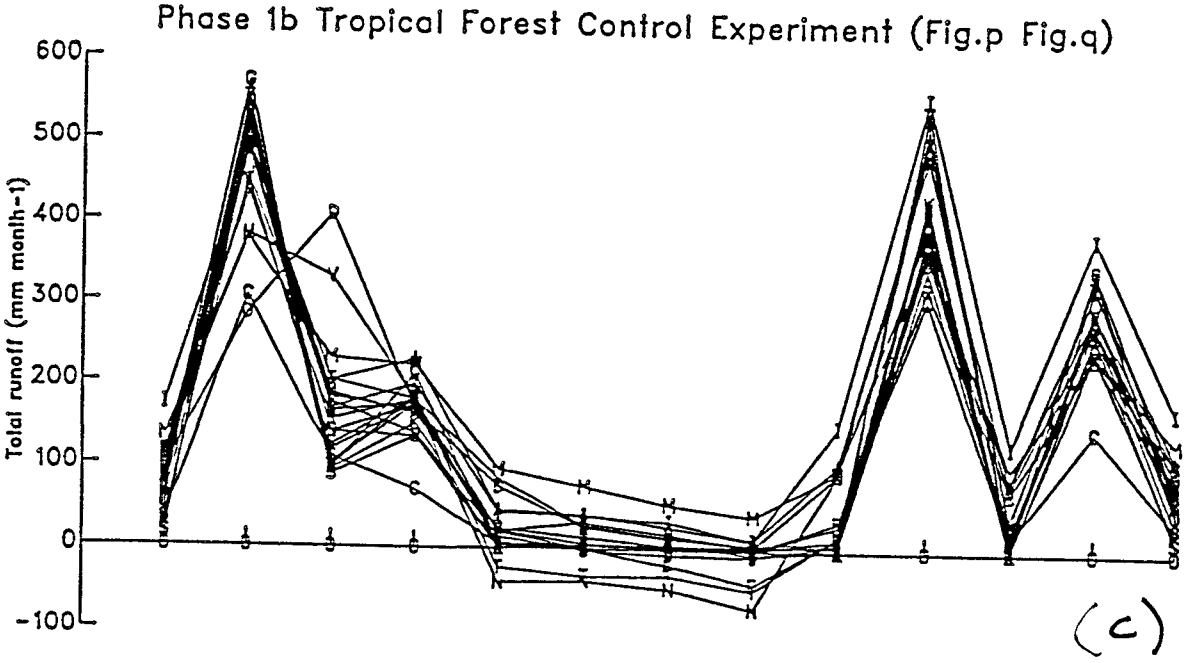
Phase 1b Tropical Forest Control Experiment (Fig.p Fig.q)
Total runoff (mm month-1)
600
500
400
300
200
100
0
-100
(c)

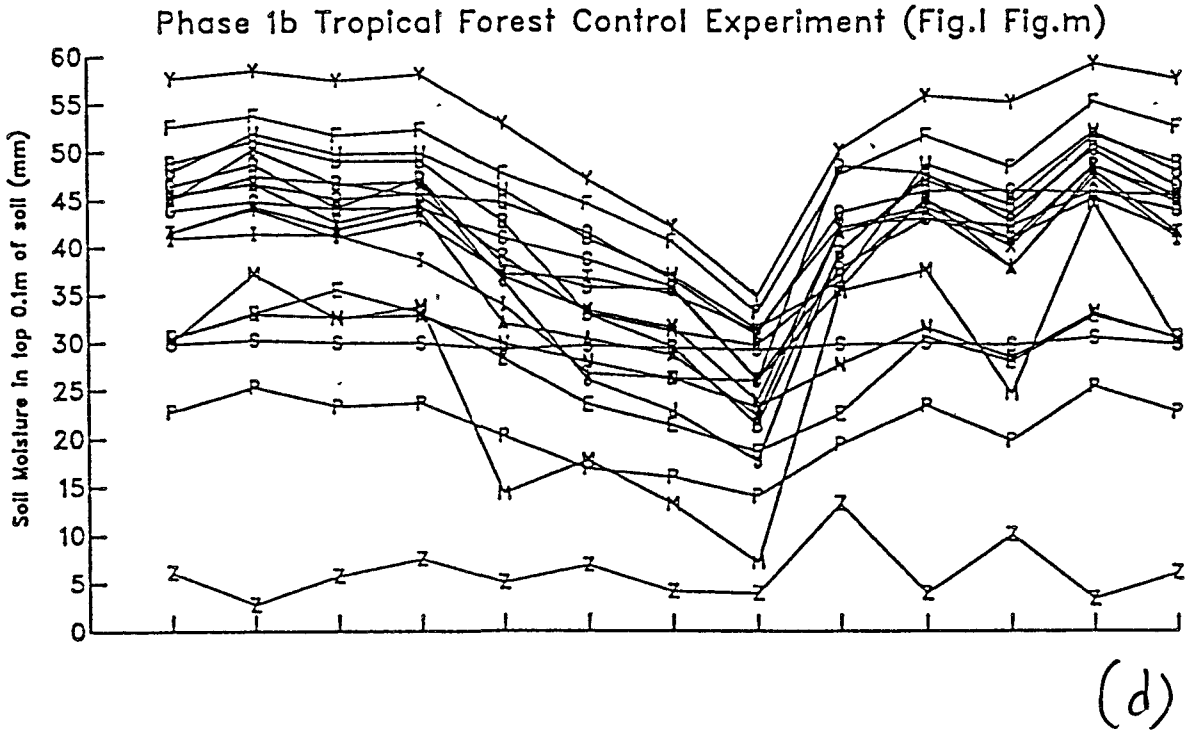
Phase 1b Tropical Forest Control Experiment (Fig.l Fig.m)
Soil Moisture in top 0.1m of soil (mm)
60
55
50
45
40
35
30
25
20
15
10
5
0
(d)

Fig. 2.5 (c), (d)